

Can dark matter be a Bose-Einstein condensate?

C. G. Böhrer*

Institute of Cosmology & Gravitation, University of Portsmouth, Portsmouth PO1 2EG, UK

T. Harko†

*Department of Physics and Center for Theoretical and Computational Physics,
The University of Hong Kong, Pok Fu Lam Road, Hong Kong*

(Dated: November 26, 2024)

We consider the possibility that the dark matter, which is required to explain the dynamics of the neutral hydrogen clouds at large distances from the galactic center, could be in the form of a Bose-Einstein condensate. To study the condensate we use the non-relativistic Gross-Pitaevskii equation. By introducing the Madelung representation of the wave function, we formulate the dynamics of the system in terms of the continuity equation and of the hydrodynamic Euler equations. Hence dark matter can be described as a non-relativistic, Newtonian Bose-Einstein gravitational condensate gas, whose density and pressure are related by a barotropic equation of state. In the case of a condensate with quartic non-linearity, the equation of state is polytropic with index $n = 1$. In the framework of the Thomas-Fermi approximation the structure of the Newtonian gravitational condensate is described by the Lane-Emden equation, which can be exactly solved. General relativistic configurations with quartic non-linearity are studied, by numerically integrating the structure equations. The basic parameters (mass and radius) of the Bose-Einstein condensate dark matter halos sensitively depend on the mass of the condensed particle and of the scattering length. To test the validity of the model we fit the Newtonian tangential velocity equation of the model with a sample of rotation curves of low surface brightness and dwarf galaxies, respectively. We find a very good agreement between the theoretical rotation curves and the observational data for the low surface brightness galaxies. The deflection of photons passing through the dark matter halos is also analyzed, and the bending angle of light is computed. The bending angle obtained for the Bose-Einstein condensate is larger than that predicted by standard general relativistic and dark matter models. The angular radii of the Einstein rings are obtained in the small angles approximation. Therefore the study of the light deflection by galaxies and the gravitational lensing could discriminate between the Bose-Einstein condensate dark matter model and other dark matter models.

PACS numbers: 04.50.+h, 04.20.Jb, 04.20.Cv, 95.35.+d

I. INTRODUCTION

The existence of the dark matter in the Universe is a well established observational fact. The rotation curves of spiral galaxies [1] are one of the best evidences showing a modified gravitational particle dynamic at galactic level. In these galaxies neutral hydrogen clouds are observed at large distances from the center, much beyond the extent of the luminous matter. Assuming a non-relativistic Doppler effect and emission from stable circular orbits in a Newtonian gravitational field, the frequency shifts in the 21 cm line hydrogen emission lines allows the measurement of the velocity of the clouds. Since the clouds move in circular orbits with velocity $v_{tg}(r)$, the orbits are maintained by the balance between the centrifugal acceleration v_{tg}^2/r and the gravitational attraction force $GM(r)/r^2$ of the total mass $M(r)$ contained within the orbit. This allows the expression of the mass profile of the galaxy in the form $M(r) = rv_{tg}^2/G$.

Observations show that the rotational velocities increase near the center of the galaxy and then remain nearly constant at a value of $v_{tg\infty} \sim 200$ km/s [1]. This leads to a mass profile $M(r) = rv_{tg\infty}^2/G$. Consequently, the mass within a distance r from the center of the galaxy increases linearly with r , even at large distances where very little luminous matter can be detected.

Several theoretical models, based on a modification of Newton's law or of general relativity, have been proposed to explain the behavior of the galactic rotation curves. A modified gravitational potential of the form $\phi = -GM[1 + \alpha \exp(-r/r_0)] / (1 + \alpha)r$, with $\alpha = -0.9$ and $r_0 \approx 30$ kpc can explain flat rotational curves for most of the galaxies [2].

*Electronic address: christian.boehmer@port.ac.uk

†Electronic address: harko@hkucc.hku.hk

In an other model, called MOND, and proposed by Milgrom [3], the Poisson equation for the gravitational potential $\nabla^2\phi = 4\pi G\rho$ is replaced by an equation of the form $\nabla[\mu(x)(|\nabla\phi|/a_0)] = 4\pi G\rho$, where a_0 is a fixed constant and $\mu(x)$ a function satisfying the conditions $\mu(x) = x$ for $x \ll 1$ and $\mu(x) = 1$ for $x \gg 1$. The force law, giving the acceleration a of a test particle becomes $a = a_N$ for $a_N \gg a_0$ and $a = \sqrt{a_N a_0}$ for $a_N \ll a_0$, where a_N is the usual Newtonian acceleration. The rotation curves of the galaxies are predicted to be flat, and they can be calculated once the distribution of the baryonic matter is known. Alternative theoretical models to explain the galactic rotation curves have been elaborated recently by Mannheim [4], Moffat and Sokolov [5] and Roberts [6]. The idea that dark matter is a result of the bulk effects in brane world cosmological models was considered in [7].

A general analysis of the possibility of an alternative gravity theory explaining the dynamics of galactic systems without dark matter was performed by Zhytnikov and Nester [8]. From very general assumptions about the structure of a relativistic gravity theory (the theory is metric, invariant under general coordinates transformation, has a good linear approximation, it does not possess any unusual gauge freedom and it is not a higher derivative gravity), a general expression for the metric to order $(v/c)^2$ has been derived. This allows to compare the predictions of the theory with various experimental data: the Newtonian limit, light deflection and retardation, rotation of galaxies and gravitational lensing. The general conclusion of this study is that the possibility for any gravity theory to explain the behavior of galaxies without dark matter is rather improbable.

Hence one of most promising ways to explain the galactic rotation curves is by postulating the existence of some dark (invisible) matter, distributed in a spherical halo around the galaxies. This behavior of the galactic rotation curves is explained by postulating the existence of some dark (invisible) matter, distributed in a spherical halo around the galaxies. The dark matter is assumed to be a cold, pressure-less medium. There are many possible candidates for dark matter, the most popular ones being the weakly interacting massive particles (WIMP) (for a recent review of the particle physics aspects of dark matter see [9]). Their interaction cross section with normal baryonic matter, while extremely small, are expected to be non-zero and we may expect to detect them directly. It has also been suggested that the dark matter in the Universe might be composed of superheavy particles, with mass $\geq 10^{10}$ GeV. But observational results show the dark matter can be composed of superheavy particles only if these interact weakly with normal matter or if their mass is above 10^{15} GeV [10]. Scalar fields or other long range coherent fields coupled to gravity have also intensively been used to model galactic dark matter [11].

At very low temperatures, particles in a dilute Bose gas can occupy the same quantum ground state, forming a Bose-Einstein (BEC) condensate, which appears as a sharp peak over a broader distribution in both coordinates and momentum space. The possibility to obtain quantum degenerate gases by a combination of laser and evaporative cooling techniques has opened several new lines of research, at the border of atomic, statistical and condensed matter physics (for recent reviews see [12, 13]).

An ideal system for the experimental observation of the BEC condensation is a dilute atomic Bose gas confined in a trap and cooled to very low temperatures. BEC were first observed in 1995 in dilute alkali gases such as vapors of rubidium and sodium. In these experiments, atoms were confined in magnetic traps, evaporatively cooled down to a fraction of a microkelvin, left to expand by switching off the magnetic trap, and subsequently imaged with optical methods. A sharp peak in the velocity distribution was observed below a critical temperature, indicating that condensation has occurred, with the alkali atoms condensed in the same ground state. Under the typical confining conditions of experimental settings, BEC's are inhomogeneous, and hence condensates arise as a narrow peak not only in the momentum space but also in the coordinate space [14].

If considering only two-body, mean field interactions, a dilute Bose-Einstein gas near zero temperature can be modeled using a cubic non-linear Schrödinger equation with an external potential, which is known as the Gross-Pitaevskii equation [12].

The idea that the dark matter is composed of ultra-light scalar particles ($m \approx 10^{-22}$ eV) in a (cold) Bose-Einstein condensate state, was proposed initially in [15], and further developed in [16]. The wave properties of the dark matter stabilize gravitational collapse, providing halo cores and sharply suppressing small-scale linear power. The speed of BEC's in atomic vapors and in galactic dark matter was studied in [17]. A cosmological model in which the boson dark matter gradually condensates into dark energy was considered in [18]. Negative pressure associated with the condensate yields the accelerated expansion of the Universe and the rapid collapse of the smallest scale fluctuations into many black holes, which become the seeds of the first galaxies.

Scalar mediated interactions among baryons embedded in a Bose-Einstein condensate, composed of the mediating particles, which extend well beyond the Compton wavelength, were studied in [19]. If the dark matter of the Universe is composed of such a condensate, the imprints of an interaction between the baryonic and the dark matter could be manifest as anomalies in the peak structure of the Cosmic Microwave Background. In a medium composed of scalar particles with non-zero mass, the range of Van der Waals-type scalar mediated interactions among nucleons becomes infinite when the medium makes a transition to a Bose-Einstein condensed phase. In an astrophysical context this phenomenon was explored in [20] and the effect of a scalar dark matter background on the equilibrium of degenerate stars was studied.

A relativistic version of the Gross-Pitaevskii equation was proposed in [21] and the cosmological implications of a steady slow BEC process were considered. It is interesting to note that the resulting equation of state for the condensate is that of the Whittaker solution [22], which has special importance in classical general relativity. Namely, the solution is the static non-rotating limit of the Wahlquist solution, which is probably the most important exact rotating perfect fluid spacetime.

Dolgov and Smirnov [23] assumed that the Pauli exclusion principle is violated for neutrinos, and consequently, neutrinos obey the Bose-Einstein statistics. Neutrinos may form cosmological Bose condensates, which accounts for all (or a part of) the dark matter in the universe. “Wrong” statistics of neutrinos could modify big bang nucleosynthesis, leading to the effective number of neutrino species smaller than three. The Pauli principle violation for neutrinos can be tested in the two-neutrino double beta decay. In order to effectively modify Kepler’s law without changing standard Newtonian gravity, the galactic dark matter was described by a scalar field in [24]. For cold scalar fields, this model corresponds to a gravitationally confined Boson-Einstein condensate, but of galactic dimensions. A light, neutral vector particle associated with a vector field ϕ^μ , and which appears in a modified theory of gravity, may form a cold fluid of Bose-Einstein condensates before the cosmological recombination with zero pressure and zero shear viscosity [25]. Vortices in axion condensates on the galactic scale have been studied in [26]. Such vortices can occur as a result of global rotation of the early universe. Various cosmological implications of axion condensation have been investigated in [27].

The dynamical equations describing the evolution of a self-gravitating fluid of cold dark matter can be written in the form of a Schrodinger equation coupled to a Poisson equation, describing Newtonian gravity. It has been shown that, in the quasi-linear regime, the Schrodinger equation can be reduced to the exactly solvable free-particle Schrodinger equation. This approach can be used to study gravitational instabilities or structure formation [28]. Unified models for dark matter and dark energy via a single fluid and models discussing the properties of the dark energy and cosmological horizons have been proposed and discussed in [29].

It is the purpose of the present paper to systematically investigate the possibility that the dark matter, which is required to explain the dynamics of the neutral hydrogen clouds at large distances from the galactic center, could be in the form of a Bose-Einstein condensate. To study the dark matter condensate we use the non-relativistic Gross-Pitaevskii equation. By introducing the Madelung representation of the wave function, we formulate the dynamics of the (quantum) system in terms of the continuity equation and of the hydrodynamic Euler equations. Hence dark matter can be described as a non-relativistic, Newtonian Bose-Einstein gravitational condensate gas, whose density and pressure are related by a barotropic equation of state. In the case of a condensate with quartic non-linearity, the equation of state is polytropic with index $n = 1$.

In the framework of the Thomas-Fermi approximation, the structure of the Newtonian gravitational condensate is described by the Lane-Emden equation, which can be exactly solved. General relativistic configurations with quartic non-linearity are studied, by numerically integrating the structure equations. The basic parameters (mass and radius) of the Bose-Einstein condensate dark matter halos sensitively depend on the mass m of the condensed particle, of the scattering length a and of the central density of the dark matter. The values of these parameters can be constrained by using the known radii and masses of the galactic dark matter halos.

To test the viability of the model and in order to apply it to realistic systems, we compute the rotation curve of the Bose-Einstein condensate for a sample of 12 galaxies that includes low surface brightness and dwarf galaxies with measured rotation curves extending in the dark matter dominated region. A best fit to the rotation curves of galaxies is obtained in terms of a parametric core baryonic mass distribution, which is superposed with the Bose-Einstein condensate mass distribution. It turns out that the Newtonian potential of the core is asymptotically decreasing, but the corrected rotation curve is much higher than the Newtonian one, thus offering the possibility to fit the rotation curves. For low surface brightness galaxies we find a very good agreement between the theoretical rotation curve with a normal baryonic core and the observational data.

The deflection of photons passing through the dark matter halos is also analyzed, and the bending angle of light is computed. The bending angle obtained for the Bose-Einstein condensate is larger than that predicted by standard general relativistic and dark matter models. The angular radii of the Einstein rings are obtained in the small angles approximation. Therefore the study of the light deflection by galaxies and the gravitational lensing provides a powerful observational method to discriminate between the Bose-Einstein condensate dark matter model and other dark matter models.

The present paper is organized as follows. The basic equations describing the gravitationally bounded Bose-Einstein condensate are derived in Section II. The case of the condensate with quartic non-linearity is considered in Section III. Newtonian dark matter condensate models are analyzed in Section IV. General relativistic condensate models are studied numerically in Section V. We compare the predictions of our model with the observed galactic rotation curves in Section VI. The bending of light by dark matter condensate halos is considered in Section VII. We discuss and conclude our results in Section VIII.

II. THE GROSS-PITAEVSKII EQUATION FOR GRAVITATIONALLY BOUNDED BOSE-EINSTEIN CONDENSATES

In a quantum system of N interacting condensed bosons most of the bosons lie in the same single-particle quantum state. For a system consisting of a large number of particles, the calculation of the ground state of the system with the direct use of the Hamiltonian is impracticable, due to the high computational cost. However, the use of some approximate methods can lead to a significant simplification of the formalism. One such approach is the mean field description of the condensate, which is based on the idea of separating out the condensate contribution to the bosonic field operator. We also assume that in a medium composed of scalar particles with non-zero mass, the range of Van der Waals-type scalar mediated interactions among nucleons becomes infinite, when the medium makes a transition to a Bose-Einstein condensed phase.

The many-body Hamiltonian describing the interacting bosons confined by an external potential V_{ext} is given, in the second quantization, by

$$\hat{H} = \int d\vec{r} \hat{\Psi}^+(\vec{r}) \left[-\frac{\hbar^2}{2m} \nabla^2 + V_{rot}(\vec{r}) + V_{ext}(\vec{r}) \right] \hat{\Psi}(\vec{r}) + \frac{1}{2} \int d\vec{r} d\vec{r}' \hat{\Psi}^+(\vec{r}) \hat{\Psi}^+(\vec{r}') V(\vec{r} - \vec{r}') \hat{\Psi}(\vec{r}) \hat{\Psi}(\vec{r}'), \quad (1)$$

where $\hat{\Psi}(\vec{r})$ and $\hat{\Psi}^+(\vec{r})$ are the boson field operators that annihilate and create a particle at the position \vec{r} , respectively, and $V(\vec{r} - \vec{r}')$ is the two-body interatomic potential [12]. $V_{rot}(\vec{r})$ is the potential associated to the rotation of the condensate, and is given by

$$V_{rot}(\vec{r}) = f_{rot}(t) \frac{m\omega^2}{2} \vec{r}^2, \quad (2)$$

where ω is the angular velocity of the condensate and $f_{rot}(t)$ a function which takes into account the possible time variation of the rotation potential. For a system consisting of a large number of particles, the calculation of the ground state of the system with the direct use of Eq. (1) is impracticable, due to the high computational cost.

Therefore, the use of some approximate methods can lead to a significant simplification of the formalism. One such approach is the mean field description of the condensate, which is based on the idea of separating out the condensate contribution to the bosonic field operator. For a uniform gas in a volume V , BEC occurs in the single particle state $\Psi_0 = 1/\sqrt{V}$, having zero momentum. The field operator can be decomposed then in the form $\hat{\Psi}(\vec{r}) = \sqrt{N/V} + \hat{\Psi}'(\vec{r})$. By treating the operator $\hat{\Psi}'(\vec{r})$ as a small perturbation, one can develop the first order theory for the excitations of the interacting Bose gases [12].

In the general case of a non-uniform and time-dependent configuration the field operator in the Heisenberg representation is given by

$$\hat{\Psi}(\vec{r}, t) = \psi(\vec{r}, t) + \hat{\Psi}'(\vec{r}, t), \quad (3)$$

where $\psi(\vec{r}, t)$, also called the condensate wave function, is the expectation value of the field operator, $\psi(\vec{r}, t) = \langle \hat{\Psi}(\vec{r}, t) \rangle$. It is a classical field and its absolute value fixes the number density of the condensate through $\rho(\vec{r}, t) = |\psi(\vec{r}, t)|^2$. The normalization condition is $N = \int \rho(\vec{r}, t) d^3\vec{r}$, where N is the total number of particles in the condensate.

The equation of motion for the condensate wave function is given by the Heisenberg equation corresponding to the many-body Hamiltonian given by Eq. (1),

$$i\hbar \frac{\partial}{\partial t} \hat{\Psi}(\vec{r}, t) = [\hat{\Psi}, \hat{H}] = \left[-\frac{\hbar^2}{2m} \nabla^2 + V_{rot}(\vec{r}) + V_{ext}(\vec{r}) + \int d\vec{r}' \hat{\Psi}^+(\vec{r}', t) V(\vec{r}' - \vec{r}) \hat{\Psi}(\vec{r}', t) \right] \hat{\Psi}(\vec{r}, t). \quad (4)$$

By replacing $\hat{\Psi}(\vec{r}, t)$ with the condensate wave function ψ gives the zeroth-order approximation to the Heisenberg equation. In the integral containing the particle-particle interaction $V(\vec{r}' - \vec{r})$ this replacement is in general a poor approximation for short distances. However, in a dilute and cold gas, only binary collisions at low energy are relevant and these collisions are characterized by a single parameter, the s -wave scattering length, independently of the details of the two-body potential. Therefore, one can replace $V(\vec{r}' - \vec{r})$ with an effective interaction $V(\vec{r}' - \vec{r}) = \lambda \delta(\vec{r}' - \vec{r})$, where the coupling constant λ is related to the scattering length a through $\lambda = 4\pi\hbar^2 a/m$. Hence, we assume that in a medium composed of scalar particles with non-zero mass, the range of Van der Waals-type scalar mediated interactions among nucleons becomes infinite, when the medium makes a transition to a Bose-Einstein condensed phase.

With the use of the effective potential the integral in the bracket of Eq. (4) gives $\lambda |\psi(\vec{r}, t)|^2$, and the resulting equation is the Schrodinger equation with a quartic nonlinear term [12].

However, in order to obtain a more general description of the Bose-Einstein condensate stars, we shall assume an arbitrary non-linear term $g \left(|\psi(\vec{r}, t)|^2 \right)$ [30], where we have denoted

$$\rho = |\psi(\vec{r}, t)|^2. \quad (5)$$

The probability density ρ is normalized according to $\int d^3\vec{r}\rho = N$. As was pointed out in [31], the Gross-Pitaevskii approximation is a long-wavelength theory widely used to describe a variety of properties of dilute Bose condensates, but for short-ranged repulsive interactions this theory fails in low dimensions, and some essential modifications of the theory are necessary.

Therefore the generalized Gross-Pitaevskii equation describing a gravitationally trapped rotating Bose-Einstein condensate is given by

$$i\hbar\frac{\partial}{\partial t}\psi(\vec{r}, t) = \left[-\frac{\hbar^2}{2m}\nabla^2 + V_{rot}(\vec{r}) + V_{ext}(\vec{r}) + g' \left(|\psi(\vec{r}, t)|^2 \right) \right] \psi(\vec{r}, t), \quad (6)$$

where we denoted $g' = dg/d\rho$. The mass of the condensed particles is denoted by m .

As for $V_{ext}(\vec{r})$, we assume that it is the gravitational potential V , $V_{ext} = V$, and it satisfies the Poisson equation

$$\nabla^2 V = 4\pi G\rho_m, \quad (7)$$

where $\rho_m = m\rho$ is the mass density inside the Bose-Einstein condensate.

The physical properties of a Bose-Einstein condensate described by the generalized Gross-Pitaevskii equation given by Eq. (6) can be understood much easily by using the so-called Madelung representation of the wave function [32], which consist in writing ψ in the form

$$\psi(\vec{r}, t) = \sqrt{\rho(\vec{r}, t)} \exp \left[\frac{i}{\hbar} S(\vec{r}, t) \right], \quad (8)$$

where the function $S(\vec{r}, t)$ has the dimensions of an action.

By substituting the above expression of the wave function into Eq. (6) it decouples into a system of two differential equations for the real functions ρ and \vec{v} , given by

$$\frac{\partial\rho_m}{\partial t} + \nabla \cdot (\rho_m \vec{v}) = 0, \quad (9)$$

$$\rho_m \left[\frac{\partial\vec{v}}{\partial t} + (\vec{v} \cdot \nabla) \vec{v} \right] = -\nabla P \left(\frac{\rho_m}{m} \right) - \rho_m \nabla \left(\frac{V_{rot}}{m} \right) - \rho_m \nabla \left(\frac{V_{ext}}{m} \right) - \nabla \cdot \sigma^Q, \quad (10)$$

where we have introduced the quantum potential

$$V_Q = -\frac{\hbar^2}{2m} \frac{\nabla^2 \sqrt{\rho}}{\sqrt{\rho}}, \quad (11)$$

the velocity of the quantum fluid

$$\vec{v} = \frac{\nabla S}{m}, \quad (12)$$

respectively, and we denoted

$$P \left(\frac{\rho_m}{m} \right) = g' \left(\frac{\rho_m}{m} \right) \frac{\rho_m}{m} - g \left(\frac{\rho_m}{m} \right). \quad (13)$$

From its definition it follows that the velocity field is irrotational, satisfying the condition $\nabla \times \vec{v} = 0$.

The quantum potential V_Q has the property [32]

$$\rho \nabla_i V_Q = \nabla_j \left(-\frac{\hbar^2}{4m} \rho \nabla_i \nabla_j \ln \rho \right) = \nabla_j \sigma_{ij}^Q, \quad (14)$$

where $\sigma_{ij}^Q = -\hbar^2 \rho \nabla_i \nabla_j \ln \rho / 4m$ is the quantum stress tensor, which has the dimensions of a pressure and is an intrinsically anisotropic quantum contribution to the equations of motion.

Therefore the equations of motion of the gravitational ideal Bose-Einstein condensate take the form of the equation of continuity and of the hydrodynamic Euler equations. The Bose-Einstein gravitational condensate can be described as a gas whose density and pressure are related by a barotropic equation of state [30]. The explicit form of this equation depends on the form of the non-linearity term g .

For a static ideal condensate, $\vec{v} \equiv 0$. In this case from Eq. (10) we obtain

$$V_Q + V_{rot} + V_{ext} + g' = \text{constant} \quad (15)$$

By applying the operator ∇^2 to both sides of Eq. (15) gives

$$\nabla^2 (V_Q + V_{rot} + g') + \nabla^2 V_{ext} = 0. \quad (16)$$

In the case of a condensate with a non-linearity of the form $g(\rho_m) = k\rho_m^2/2$ and in the presence of a confining gravitational field $V = V_{ext}$, it follows that the generalized potential $V_{gen} = -V_Q - V_{rot} - k\rho_m$ satisfies the Poisson equation,

$$\nabla^2 V_{gen} = 4\pi G\rho_m. \quad (17)$$

If the quantum potential can be neglected, the mass density of the condensate is described by the Helmholtz type equation

$$\nabla^2 \rho_m + \frac{4\pi G}{k} \rho_m + \frac{\omega^2}{k} = 0. \quad (18)$$

III. STATIC AND SLOWLY ROTATING NEWTONIAN BOSE-EINSTEIN CONDENSATES

When the number of particles in the gravitationally bounded Bose-Einstein condensate becomes large enough, the quantum pressure term makes a significant contribution only near the boundary of the condensate. Hence it is much smaller than the non-linear interaction term. Thus the quantum stress term in the equation of motion of the condensate can be neglected. This is the Thomas-Fermi approximation, which has been extensively used for the study of the Bose-Einstein condensates [12]. As the number of particles in the condensate becomes infinite, the Thomas-Fermi approximation becomes exact [33]. This approximation also corresponds to the classical limit of the theory (it corresponds to neglecting all terms with powers of \hbar or as the regime of strong repulsive interactions among particles. From a mathematical point of view the Thomas-Fermi approximation corresponds to neglecting in the equation of motion all terms containing $\nabla\rho$ and ∇S .

In the case of a static Bose-Einstein condensate, all physical quantities are independent of time. Moreover, in the first approximation we also neglect the rotation of the condensate, taking $V_{rot} = 0$. Therefore the equations describing the static Bose-Einstein condensate in a gravitational field with potential V take the form

$$\nabla P \left(\frac{\rho_m}{m} \right) = -\rho_m \nabla \left(\frac{V}{m} \right), \quad (19)$$

$$\nabla^2 V = 4\pi G\rho_m. \quad (20)$$

These equations must be integrated together with the equation of state $P = P(\rho_m)$, which follows from Eq. (13), and some appropriately chosen boundary conditions. By assuming that the non-linearity in the Gross-Pitaevskii equation is of the form

$$g(\rho) = \alpha\rho^\Gamma, \quad (21)$$

where α and Γ are positive constants, $\alpha = \text{constant} > 0$, $\Gamma = \text{constant} > 0$, it follows that the equation of state of the gravitational Bose-Einstein condensate is the polytropic equation of state,

$$P(\rho_m) = \alpha(\Gamma - 1)\rho_m^\Gamma = K\rho_m^\Gamma, \quad (22)$$

where we denoted $K = \alpha(\Gamma - 1)$.

By representing Γ in the form $\Gamma = 1 + 1/n$, where n is the polytropic index, it follows that the structure of the static gravitationally bounded Bose-Einstein condensate is described by the Lane-Emden equation,

$$\frac{1}{\xi^2} \frac{d}{d\xi} \left(\xi^2 \frac{d\theta}{d\xi} \right) + \theta^n = 0, \quad (23)$$

where θ is a dimensionless variable defined via $\rho_m = \rho_{cm}\theta^n$ and ξ is a dimensionless coordinate introduced via the transformation $r = \left[(n+1)K\rho_{cm}^{1/n-1}/4\pi G \right]^{1/2} \xi$. ρ_{cm} is the central density of the condensate [34].

Hence the mass and the radius of the condensate are given by

$$R = \left[\frac{(n+1)\alpha}{4\pi Gn} \right]^{1/2} \rho_{cm}^{(1-n)/2} \xi_1, \quad (24)$$

and

$$M = 4\pi \left[\frac{(n+1)\alpha}{4\pi Gn} \right]^{3/2} \rho_{cm}^{(3-n)/2n} \xi_1^2 |\theta'(\xi_1)|, \quad (25)$$

respectively, where ξ_1 defines the zero-pressure and zero-density surface of the condensate, $\theta(\xi_1) = 0$ [34].

In the standard approach to the Bose-Einstein condensates, the non-linearity term g is given by

$$g(\rho) = \frac{u_0}{2} |\psi|^4 = \frac{u_0}{2} \rho^2, \quad (26)$$

where $u_0 = 4\pi\hbar^2 a/m$ [12]. The corresponding equation of state of the condensate is

$$P(\rho_m) = U_0 \rho_m^2, \quad (27)$$

with

$$U_0 = \frac{2\pi\hbar^2 a}{m^3}. \quad (28)$$

Therefore the equation of state of the Bose-Einstein condensate with quartic non-linearity is a polytrope with index $n = 1$. In this case the solution of the Lane-Emden equation can be obtained in an analytical form, and the solution satisfying the boundary condition $\theta(0) = 1$ is [34]

$$\theta(\xi) = \frac{\sin \xi}{\xi}. \quad (29)$$

The radius of the gravitationally bounded system is defined by the condition $\theta(\xi_1) = 0$, giving $\xi_1 = \pi$. Therefore the radius R of the Bose-Einstein condensate is given by

$$R = \pi \sqrt{\frac{\hbar^2 a}{Gm^3}}. \quad (30)$$

The radius of the gravitationally bounded Bose-Einstein condensate with quartic non-linearity is independent of the central density and the mass of the system, and depends only on the physical characteristics of the condensate.

The total mass of the condensate is obtained as

$$M = 4\pi^3 \left(\frac{\hbar^2 a}{Gm^3} \right)^{3/2} \rho_{cm} |\theta'(\xi_1)| = 4\pi^2 \left(\frac{\hbar^2 a}{Gm^3} \right)^{3/2} \rho_{cm}, \quad (31)$$

where we have used $|\theta'(\xi_1)| = 1/\pi$.

The mass-radius relation for the static condensate is given by

$$M = \frac{4}{\pi} R^3 \rho_{cm}, \quad (32)$$

which shows that the mean density of the condensate $\langle \rho_m \rangle = 3M/4\pi R^3$ can be obtained from the central density of the condensate by the relation

$$\langle \rho_m \rangle = 3 \frac{\rho_{cm}}{\pi^2}. \quad (33)$$

The case of the slowly rotating Bose-Einstein condensates can also be straightforwardly analyzed, by taking into account the fact that the condensate obeys a polytropic equation of state. The study of the slowly rotating polytropes was performed in detail by Chandrasekhar [35].

The Lane-Emden equation for a rotating Bose-Einstein condensate is

$$\frac{1}{\xi^2} \frac{\partial}{\partial \xi} \left(\xi^2 \frac{\partial \theta}{\partial \xi} \right) + \frac{1}{\xi^2} \frac{\partial}{\partial \mu} \left[(1 - \mu^2) \frac{\partial \theta}{\partial \mu} \right] = -\theta^n + \Omega, \quad (34)$$

where $\mu = \cos \theta$ and $\Omega = \omega^2 / 2\pi G \rho_{cm}$. The radius R_ω and the mass M_ω of the condensate in slow rotation are given in the first order in Ω by

$$R_\omega = \left[\frac{(n+1)\alpha}{4\pi G n} \right]^{1/2} \rho_{cm}^{(1-n)/2} \xi_1 \left[1 + \frac{3\psi_0(\xi_1)}{\xi_1 |\theta'(\xi_1)|} \Omega \right]^{1/3}, \quad (35)$$

and

$$M_\omega = 4\pi \left[\frac{(n+1)\alpha}{4\pi G n} \right]^{3/2} \rho_{cm}^{(3-n)/2n} \xi_1^2 |\theta'(\xi_1)| \left[1 + \frac{\xi_1/3 - \psi'_0(\xi_1)}{|\theta'(\xi_1)|} \Omega \right], \quad (36)$$

respectively. The values of the function ψ_0 are tabulated in [35].

In the case of the Bose-Einstein condensate with quartic non-linearity, with polytropic index $n = 1$, the Lane-Emden equation can be integrated exactly, giving for the radius and mass of the rotating condensate the following simple relations

$$R_\omega = R (1 + 3\Omega)^{1/3}, \quad (37)$$

$$M_\omega = M \left[1 + \left(\frac{\pi^2}{3} - 1 \right) \Omega \right]. \quad (38)$$

With respect to a scaling of the parameters m , a and ρ_{cm} of the form $m \rightarrow \alpha_1 m$, $a \rightarrow \alpha_2 a$, $\rho_{cm} \rightarrow \alpha_3 \rho_{cm}$, the radius and the mass of the condensate have the following scaling properties:

$$R \rightarrow \alpha_1^{-3/2} \alpha_2^{1/2} R, M \rightarrow \alpha_1^{-9/2} \alpha_2^{3/2} \alpha_3 M. \quad (39)$$

IV. DARK MATTER AS A BOSE-EINSTEIN CONDENSATE

In the present Section we analyze, by using the results obtained in the previous Sections, the possibility that dark matter is in the form of a Bose-Einstein condensate. For simplicity we shall restrict our study to the case of a Bose-Einstein condensate with a quartic non-linearity. As a first result one has to point out that, if dark matter is a Bose-Einstein condensate, it cannot be pressure-less, as usually considered in most of the investigations of the galactic dark matter problem, but must obey a polytropic equation of state with index $n = 1$.

The possibility that dark matter has a substantial amounts of pressure, comparable in magnitude to the energy density, has been discussed in [36]. Galaxy halo models, consistent with observations of flat rotation curves, are possible for a variety of equations of state with anisotropic pressures. However, in the case of dark matter in the form of the Bose-Einstein condensate the pressure distribution is isotropic.

The density distribution of the dark matter Bose-Einstein condensate follows from Eq. (29) and is given by

$$\rho_{DM}(r) = \rho_{DM}^{(c)} \frac{\sin kr}{kr}, \quad (40)$$

where $k = \sqrt{Gm^3/\hbar^2 a}$ and $\rho_{DM}^{(c)}$ is the central density of the condensate, $\rho_{DM}^{(c)} = \rho_{DM}(0)$. The mass profile of the dark condensate galactic halo $m_{DM}(r) = 4\pi \int_0^r \rho_{DM}(r) r^2 dr$ is

$$m_{DM}(r) = \frac{4\pi \rho_{DM}^{(c)}}{k^2} r \left(\frac{\sin kr}{kr} - \cos kr \right). \quad (41)$$

Eq. (41) allows to represent the tangential velocity $v_{tg}^2(r) = Gm_{DM}(r)/r$ of a test particle moving in the dark halo as

$$v_{tg}^2(r) = \frac{4\pi G \rho_{DM}^{(c)}}{k^2} \left(\frac{\sin kr}{kr} - \cos kr \right). \quad (42)$$

For $r \rightarrow 0$ we have $v_{tg}^2(r) \rightarrow 0$.

At the boundary of the halo, which is defined by the radius R_{DM} of the halo, the density of the Bose-Einstein condensate is negligible, $\rho_{DM}(R_{DM}) = 0$ and $kr \rightarrow \pi$. These conditions give the radius of the dark matter condensate as

$$R_{DM} = \pi \sqrt{\frac{\hbar^2 a}{Gm^3}}. \quad (43)$$

The total mass of the condensate is given by

$$M_{DM} = m_{DM}(R_{DM}) = \frac{4}{\pi} R_{DM}^3 \rho_{DM}^{(c)}. \quad (44)$$

Near the vacuum boundary of the condensate the maximum tangential velocity of a test particle tends to a constant value which can be expressed as

$$v_{tg}^2(R) = \frac{4\pi G \rho_{DM}^{(c)}}{k^2} = \frac{4G \rho_{DM}^{(c)} R_{DM}^2}{\pi}. \quad (45)$$

Eqs. (40)-(45) give a complete description of the physical properties of the galactic dark matter condensates in terms of three quantities, the mass m of the condensed particle, the inter-particle scattering length a , and the central density of the condensate. Together with Eqs. (30) and (32) they can be used to constrain the physical properties of the condensate.

As a toy-model we consider the example of a galactic dark matter halo extending to up to $R_{DM} = 10$ kpc $\approx 3.08 \times 10^{22}$ cm, with a mass of the order of $M_{DM} = 3 \times 10^{11} M_{\odot}$. The mean density of the condensate dark matter is $\langle \rho_{DM} \rangle = 3M_{DM}/4\pi R_{DM}^3 \approx 5.30 \times 10^{-24}$ g/cm³. Then Eq. (33) gives the central density of the condensate as $\rho_{DM}^{(c)} = \pi^2 \langle \rho_{DM} \rangle / 3 \approx 1.74 \times 10^{-23}$ g/cm³.

An important parameter in the description of the Bose-Einstein condensate is the scattering length a . In terrestrial experiments performed with ⁸⁷Rb a has a value of the order of $a(^{87}\text{Rb}) \approx 5.77 \times 10^{-7}$ cm $\approx 5.77 \times 10^6$ fm [14]. However, for very light particles a may be much larger.

The mass of the particle in the condensate can be obtained from the radius of the dark matter halo as

$$m = \left(\frac{\pi^2 \hbar^2 a}{GR^2} \right)^{1/3} \approx 2.58 \times 10^{-30} [a(\text{cm})]^{1/3} [R(\text{kpc})]^{-2/3} \text{ g} \approx 6.73 \times 10^{-2} [a(\text{fm})]^{1/3} [R(\text{kpc})]^{-2/3} \text{ eV}. \quad (46)$$

From this equation it follows that the mass of the particle forming the condensate dark matter halos is of the order of eV. For $a \approx 1$ fm and $R \approx 10$ kpc, the mass may be of the order of $m \approx 14$ meV. For values of a of the order of $a \approx 10^6$ fm, corresponding to the values of a observed in terrestrial laboratory experiments, $m \approx 1.44$ eV. Of course much larger values of a may bring the mass of the condensate particle in the range of a few tenth of eV's.

With the use of Eq. (45) one can estimate the tangential velocity of a test particle in the dark matter halo. By using the numerical values from the previous estimations we obtain $v_{tg}(R_{DM}) \approx 365$ km/s, a value which is consistent with the observations of the galactic rotation curves. From the definition of the mean density it follows that the total mass of the condensate can be obtained from the tangential velocity as $M_{DM} \approx v_{tg}^2(R_{DM}) R_{DM} / G$.

The density profile of the Newtonian dark matter condensate and its mass profile are represented in Fig. 1.

The tangential velocity of a test particle in the gravitationally bounded galactic condensate is shown, for different values of the central density, in Fig. 2.

V. THE GENERAL RELATIVISTIC BOSE-EINSTEIN CONDENSATE GALACTIC HALOS

In the previous Sections we have considered the gravitationally bounded Bose-Einstein condensate dark matter in the framework of Newtonian gravity. General relativistic effects may change the physical properties of the dark matter condensate halos in both a qualitative and quantitative way. These effects may become particularly important since as a condensate dark matter cannot be described as a pressure-less fluid. Therefore the study of the general relativistic Bose-Einstein condensates offers a better understanding of their physical properties, and opens the possibility of direct observational testing of their properties.

For a static, spherically symmetric distribution of matter in the galactic halo the line element is

$$ds^2 = -e^{\nu(r)} c^2 dt^2 + e^{\lambda(r)} dr^2 + r^2 (d\theta^2 + \sin^2 \theta d\phi^2). \quad (47)$$

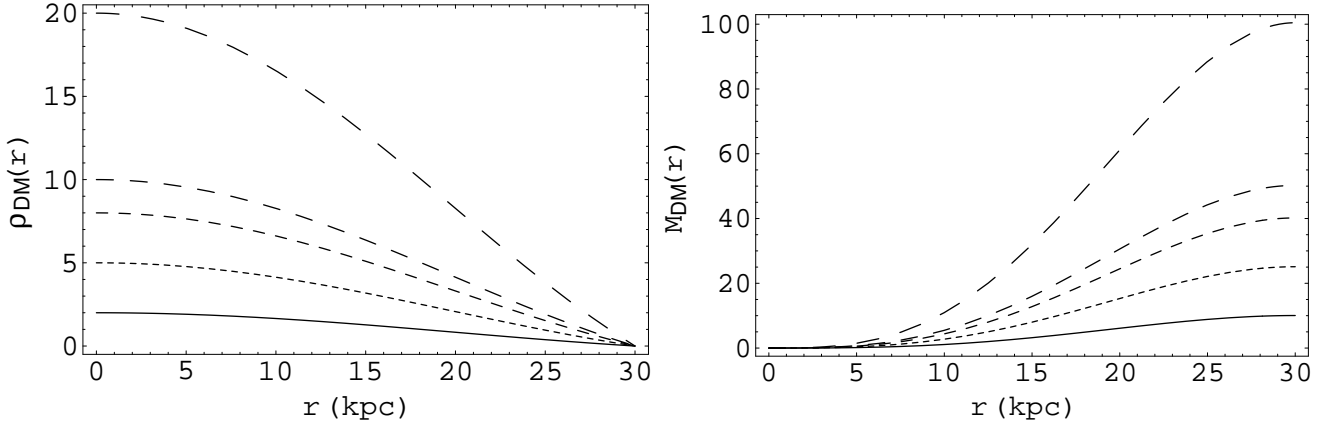


FIG. 1: Density profile (in units of 10^{-25} g/cm 3) (left figure) and mass distribution (in units of $10^{10} M_{\odot}$) (right figure) of the Newtonian Bose-Einstein condensate dark matter for different values of the central density: $\rho_{DM}^{(c)} = 2 \times 10^{-25}$ g/cm 3 (solid curve), $\rho_{DM}^{(c)} = 5 \times 10^{-25}$ g/cm 3 (dotted curve), $\rho_{DM}^{(c)} = 8 \times 10^{-25}$ g/cm 3 (short dashed curve), $\rho_{DM}^{(c)} = 1 \times 10^{-24}$ g/cm 3 (long dashed curve) and $\rho_{DM}^{(c)} = 2 \times 10^{-24}$ g/cm 3 (ultra-long dashed curve).

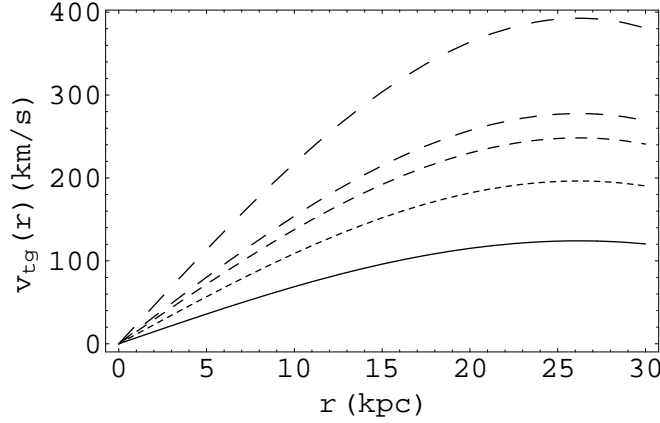


FIG. 2: Tangential velocity of a test particle in a galactic Newtonian Bose-Einstein condensate for different values of the central density: $\rho_{DM}^{(c)} = 2 \times 10^{-25}$ g/cm 3 (solid curve), $\rho_{DM}^{(c)} = 5 \times 10^{-25}$ g/cm 3 (dotted curve), $\rho_{DM}^{(c)} = 8 \times 10^{-25}$ g/cm 3 (short dashed curve), $\rho_{DM}^{(c)} = 1 \times 10^{-24}$ g/cm 3 (long dashed curve) and $\rho_{DM}^{(c)} = 2 \times 10^{-24}$ g/cm 3 (ultra-long dashed curve).

The galactic rotation curves provide the most direct method of analyzing the gravitational field inside a spiral galaxy. The rotation curves have been determined for a great number of spiral galaxies. They are obtained by measuring the frequency shifts z of the light emitted from stars and from the 21-cm radiation emission from the neutral gas clouds [1]. As shown in Appendix A, the tangential velocity of test particles in stable circular orbits is given by [37]

$$\frac{v_{tg}^2}{c^2} = \frac{r\nu'}{2}. \quad (48)$$

Thus, the rotational velocity of the test body is determined by the metric coefficient $\exp(\nu)$ only.

A general relativistic static dark matter distribution with energy density $\rho_{DM}(r)$ and pressure $P_{DM}(r)$ can be described by the mass continuity equation and by the Tolman-Oppenheimer-Volkoff (TOV) equation, which are given by [38]

$$\frac{dm_{DM}}{dr} = 4\pi\rho_{DM}r^2, \quad (49)$$

$$\frac{dP_{DM}(r)}{dr} = -\frac{(G/c^2)(\rho_{DM}c^2 + P_{DM})(4\pi P_{DM}r^3/c^2 + m_{DM})}{r^2 \left[1 - \frac{2Gm_{DM}(r)}{c^2 r}\right]}, \quad (50)$$

$$\frac{dv}{dr} = -\frac{2P'_{DM}(r)}{\rho_{DM}c^2 + P_{DM}} = \frac{2(G/c^2)(4\pi P_{DM}r^3/c^2 + m_{DM})}{r^2 \left[1 - \frac{2Gm_{DM}(r)}{c^2 r}\right]}, \quad (51)$$

where $m_{DM}(r)$ is the mass inside radius r . The system of equations (49)-(50) must be closed by choosing the equation of state for the thermodynamic pressure of the dark matter,

$$P_{DM} = P_{DM}(\rho_{DM}). \quad (52)$$

At the center of the dark matter distribution the mass must satisfy the boundary condition

$$m_{DM}(0) = 0. \quad (53)$$

For the thermodynamic pressure of the dark matter P_{DM} we assume that it vanishes on the surface of the dark halo, $P_{DM}(R) = 0$. The exterior of the Bose-Einstein condensate halo is characterized by the Schwarzschild metric, describing the vacuum outside the galaxy, and given by [38]

$$(e^\nu)^{ext} = (e^{-\lambda})^{ext} = 1 - \frac{2GM_{DM}}{r}, \quad r \geq R, \quad (54)$$

where $M_{DM} = m_{DM}(R)$ is the total mass of the dark halo. The interior solution must match with the exterior solution on the vacuum boundary of the star.

As for the equation of state of the dark matter we adopt the equation of state corresponding to the Bose-Einstein condensate with quartic nonlinearity, given by

$$P_{DM}(\rho_{DM}) = U_0 \rho_{DM}^2, \quad (55)$$

with $U_0 = 2\pi\hbar^2 a/m^3$.

The structure equations for the Bose-Einstein condensate stars can be written in a dimensionless form, by introducing a set of dimensionless variables η , M_0 , θ and Σ , respectively, and defined as

$$r = r^* \eta, \quad m_{DM} = m^* M_0, \quad \rho_{DM} = \rho_{DM}^{(c)} \theta, \quad P_{DM} = \rho_{DM}^{(c)} c^2 \lambda \theta^2, \quad (56)$$

where $\rho_{DM}^{(c)}$ is the central ($r = 0$) value of the energy density of the Bose-Einstein condensate. By taking

$$r^* = \frac{c}{\sqrt{4\pi G \rho_{DM}^{(c)}}}, \quad (57)$$

and

$$m^* = 4\pi (r^*)^3 \rho_{DM}^{(c)} = \frac{c^3}{\sqrt{4\pi G^3 \rho_{DM}^{(c)}}}, \quad (58)$$

respectively, and by denoting

$$\lambda_0 = \frac{U_0 \rho_{DM}^{(c)}}{c^2}, \quad (59)$$

the structure equations of the Bose-Einstein condensate galactic dark matter halos with quartic non-linearity can be written as

$$\frac{dM_0}{d\eta} = \theta \eta^2, \quad (60)$$

$$\frac{d\theta}{d\eta} = -\frac{(1 + \lambda_0 \theta)(\lambda_0 \theta^2 \eta^3 + M_0)}{2\lambda_0 \eta^2 \left(1 - \frac{2M_0}{\eta}\right)}, \quad (61)$$

$$\frac{d\nu}{d\eta} = -\frac{4\lambda_0}{1 + \lambda_0\theta} \frac{d\theta}{d\eta} = \frac{2(\lambda_0\theta^2\eta^3 + M_0)}{\eta^2 \left(1 - \frac{2M_0}{\eta}\right)}. \quad (62)$$

In the new dimensionless variable the boundary conditions at the center and surface of the condensate halos are given by

$$M_0(0) = 0, \quad \theta(0) = 1, \quad \theta(\eta_S) = 0, \quad (63)$$

where η_S is the value of the dimensionless radial coordinate at the vacuum boundary of the galaxy.

The general relativistic density and mass profiles of the Bose-Einstein condensate dark halos are represented, for a fixed value of m and a and for different values of the central density, in Fig. 3, respectively.

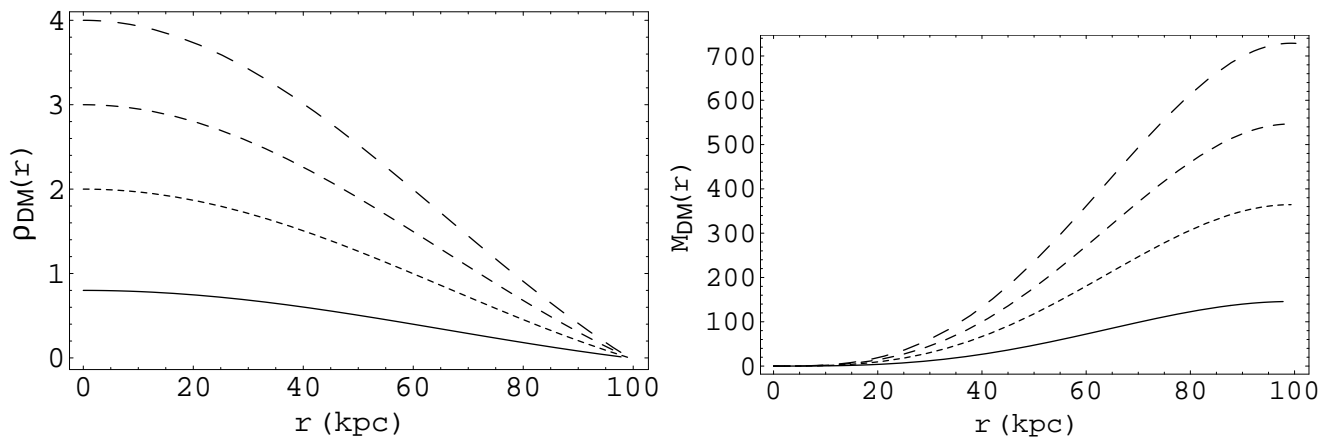


FIG. 3: General relativistic density profiles (in units of 10^{-25} g/cm³) (left figure) and mass profiles (in units of $10^{10} M_\odot$) (right figure) for a Bose-Einstein condensate galactic halo with $m = 5.6 \times 10^{-34}$ g, $a = 10^6$ fm and different values of the central density: $\rho_{DM}^{(c)} = 10^{-25}$ g/cm³ (solid curve), $\rho_{DM}^{(c)} = 2 \times 10^{-25}$ g/cm³ (dotted curve), $\rho_{DM}^{(c)} = 3 \times 10^{-25}$ g/cm³ (short dashed curve) and $\rho_{DM}^{(c)} = 4 \times 10^{-25}$ g/cm³ (long dashed curve).

The tangential velocity of a test particle moving in the dark halo is given by

$$v_{tg} = c \sqrt{\frac{\lambda_0\theta^2\eta^3 + M_0}{\eta \left(1 - \frac{2M_0}{\eta}\right)}}, \quad (64)$$

and is represented as a function of the distance to the galactic center r in Fig. 4.

For a galactic dark matter halo with mass of the order of $M_{DM} = 10^{12} M_\odot$ and radius $R_{DM} = 100$ kpc, the quantity $2GM_{DM}/c^2 R_{DM}$ is of the order of 9.6×10^{-7} , which is much smaller than one. Therefore in the nominator of Eq. (50) one can neglect the term $2Gm_{DM}(r)/c^2 r$. For central densities of the galactic halos of the order of 10^{-26} g/cm³ and for $a = 10^6$ fm, the quantity $\lambda_0 = U_0 \rho_{DM}^{(c)}/c^2 \approx 10^{-7}$, which implies $\lambda_0\theta \ll 1$.

Hence for galactic halos consisting of Bose-Einstein condensates, we can obtain a generalized Lane-Emden equation that contains the $1/c^2$ corrections

$$\frac{1}{\eta^2} \frac{d}{d\eta} \left(\eta^2 \frac{d\theta}{d\eta} \right) + \theta = \lambda_0\theta \left[-4\theta + 6\theta \frac{d\theta}{d\eta} + 5 \frac{1}{\theta} \left(\frac{d\theta}{d\eta} \right)^2 \right]. \quad (65)$$

In the zeroth order of approximation ($\lambda_0 \rightarrow 0$ which is equivalent to $c^2 \rightarrow \infty$) the resulting Lane-Emden equation reduces to the Newtonian limit Eq. (23) with $n = 1$, whose solution is given by Eq. (29). Like in the Newtonian case one can obtain a series expansion of the generalized Lane-Emden equation.

VI. COMPARING THE MODEL WITH THE OBSERVATIONAL DATA

In order to test our results we compare the predictions of our model with the observational data on the galactic rotation curves, obtained for a sample of low surface luminosity and dwarf galaxies in [39] and [40], respectively.

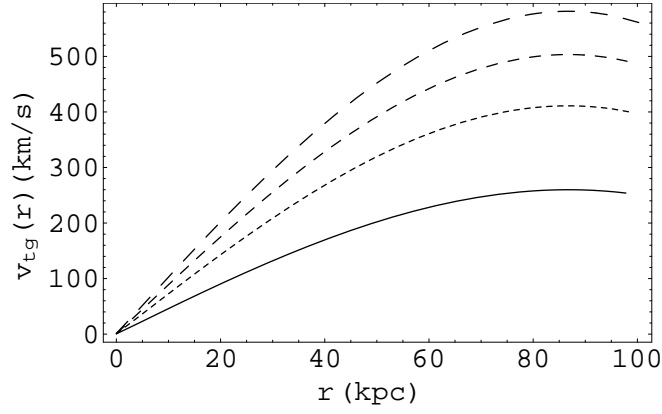


FIG. 4: Tangential velocity of a test particle in a general relativistic Bose-Einstein condensate galactic halo with $m = 5.6 \times 10^{-34}$ g, $a = 10^6$ fm for different values of the central density: $\rho_{DM}^{(c)} = 10^{-25}$ g/cm³ (solid curve), $\rho_{DM}^{(c)} = 2 \times 10^{-25}$ g/cm³ (dotted curve), $\rho_{DM}^{(c)} = 4 \times 10^{-25}$ g/cm³ (short dashed curve) and $\rho_{DM}^{(c)} = 6 \times 10^{-25}$ g/cm³ (long dashed curve).

Generally, in a realistic situation, a galaxy consists of a distribution baryonic (normal) matter, consisting of stars of mass M_{star} , ionized gas of mass M_{gas} , neutral hydrogen of mass M_{HI} etc., and the dark matter of mass M_{DM} , which we assume to be in the form of a Bose-Einstein condensate. The total mass of the galaxy is therefore $M_{tot} = M_{star} + M_{gas} + M_{HI} + M_{DM} + \dots = M_B^{tot} + M_{DM}$, where $M_B^{tot} = M_{star} + M_{gas} + M_{HI} + \dots$ is the total baryonic mass in the galaxy.

As for the baryonic mass, we assume it is concentrated into an inner core of radius r_c , and that its mass profile $M_B(r)$ can be described by the simple relation

$$M_B(r) = M_B^{tot} \left(\frac{r}{r + r_c} \right)^{3\beta}, \quad (66)$$

where $\beta = 1$ for high surface brightness galaxies (HSB) and $\beta = 2$ for low surface brightness (LSB) and dwarf galaxies, respectively [5]. Therefore the tangential velocity of a test particle in our model, in which dark matter is in a form of a Bose-Einstein condensate, is given by

$$v_{tg}^2 \text{ (km/s)} = 4.45 \times 10^4 \frac{M_B^{tot} (10^{10} M_\odot)}{r \text{ (kpc)}} \left(\frac{r}{r + r_c} \right)^{3\beta} + 8.06 \times \rho_{DM}^{(c)} (10^{-25} \text{ g/cm}^3) \times (R \text{ kpc})^2 \times \left[\frac{\sin(\pi r/R)}{\pi r/R} - \cos\left(\frac{\pi r}{R}\right) \right], \quad (67)$$

In order to test the validity of Eq. (67), which represents the basic prediction of our model, we have performed 12 galaxy rotation curves fits to a sample of low surface luminosity (LSB) galaxies and dwarf galaxies, respectively. The observational data have been taken from [39] for the LSB galaxies and from [40] for the dwarf galaxies. The fitted rotation curves are represented by a solid curve in Fig. 5, respectively, where the points represent the observational data. In all the considered cases we have adopted for β the value $\beta = 2$. The numerical results and the obtained values of the fitting parameters are summarized in Table I.

As one can see from the figure and from Table I, for 9 over 12 cases there is an overall very good agreement between the data and the best fit curve. This strongly suggest that our model may be relevant for obtaining a correct description of the dark matter and its properties. A purely Newtonian description of these observational data by assuming that the entire matter is in the form of the baryonic matter concentrated in a core region is impossible. The Newtonian potential of the core is asymptotically decreasing, but the corrected rotation curve is much higher than the Newtonian one, thus offering the possibility to fit the rotation curves. On the other hand since LSB galaxies are usually considered to be dark matter dominated, reproducing their rotation curves represents a significant evidence in favor of the model. Moreover, fitting to rotation curves allows to determine the theory parameters, and especially R , the radius of the dark matter halo, and the central density of the dark matter, $\rho_{DM}^{(c)}$. The values obtained from the fitting are physically reasonable, indicating a radius of the galactic halos in the range of 8 – 25 kpc. On the other hand, the values of the central density of the dark matter (at the galactic center) predicted by our model are of the order of 10^{-25} g/cm³, a value much smaller than the value of $\rho_{DM} (100 \text{ pc}) \approx 10 M_\odot / \text{pc}^3 \approx 7 \times 10^{-22} \text{ g/cm}^3$ estimated for our galaxy [41].

Galaxy	$M_B^{tot}/10^{10} M_\odot$	R/kpc	$\rho_{DM}^{(c)}/(10^{-25} \text{g/cm}^3)$	χ^2
DDO 189	0.39	7.88	5.51	0.33
NGC 100	0.44	8.38	10.39	1.64
NGC 1560	0.35	9.86	5.82	5.42
NGC 4395	0.71	10.22	4.81	11.07
NGC 5023	0.70	5.67	15.13	2.31
UGC 711	0.093	14.49	4.56	2.76
UGC 3371	0.17	11.22	6.12	1.92
UGC 5005	0.28	24.65	2.056	4.24
UGC/AGC 8067*	0.70	686.83	69.25	58.32
UGC/AGC 9888*	1.49	557.39	85.49	36.014
UGC 10310	0.086	8.47	9.03	0.77
UGC/AGC 241294*	0.94	950.31	54.81	61.015

TABLE I: Numerical values of the fitting parameters for the fitted rotation curves. Note that χ^2 is relatively small which suggests that our model fits the data quite well. In view of the values of χ^2 of the low luminosity dwarf galaxies, marked by *, we find that the model fits the high luminosity galaxies much better than the low luminosity ones. This is rather similar to the standard dark matter models, which also work best for high luminosity galaxies.

If our model can fit quite well the observational results for the LSB galaxies, the fits for the dwarf galaxies based on the data from [40] require an unrealistically large extension of the dark matter, and they are statistically not significant. A possible explanation may be related to the peculiar behavior of the observational data near the origin: the tangential velocities do not tend to zero for $r \rightarrow 0$, but are zero for a value of r of the order of 0.5 kpc, $v_{tg}(0.5 \text{ kpc}) \approx 0$. Thus, a possibility for a better fitting of the observational data for these galaxies would be to re-scale the radial coordinate by introducing a new parameter r_0 so that $r \rightarrow r - r_0$ and $v_{tg}(r_0) = 0$. However, the necessity of introducing a new parameter seems not to be physically motivated.

Conventionally, galactic dark matter is modelled by an isothermal sphere in hydrostatic equilibrium, having two free parameters. These parameters are adjusted for every galaxy individually. One severe problem in that approach is that it seems that the rotational velocity of the last data point scales like the luminosity. Also, the Tully-Fisher relation $L \sim v_{out}^a$, $a \approx 4$, where L is the luminosity (in units of $10^{10} L_\odot$) and v_{out} is the velocity at the outermost observed radial position, which holds for the high luminosity spiral galaxies [1], actually suggests that the luminous matter and the related Newtonian effects must play an important role in determining the rotational velocities.

VII. LIGHT DEFLECTION AND LENSING BY BOSE-EINSTEIN CONDENSATE DARK HALOS

One of the ways we could in principle test the galactic dark matter model obtained in the previous Section would be by studying the light deflection by galaxies, and in particular by studying the deflection of photons passing through the region where the rotation curves are flat. Let us consider a photon approaching a galaxy from far distances. We will compute the deflection by assuming that the metric is given by Eq. (47), together with Eqs. (60) – (62).

The bending of light by the galactic gravitational field results in a deflection angle $\Delta\phi$ given by

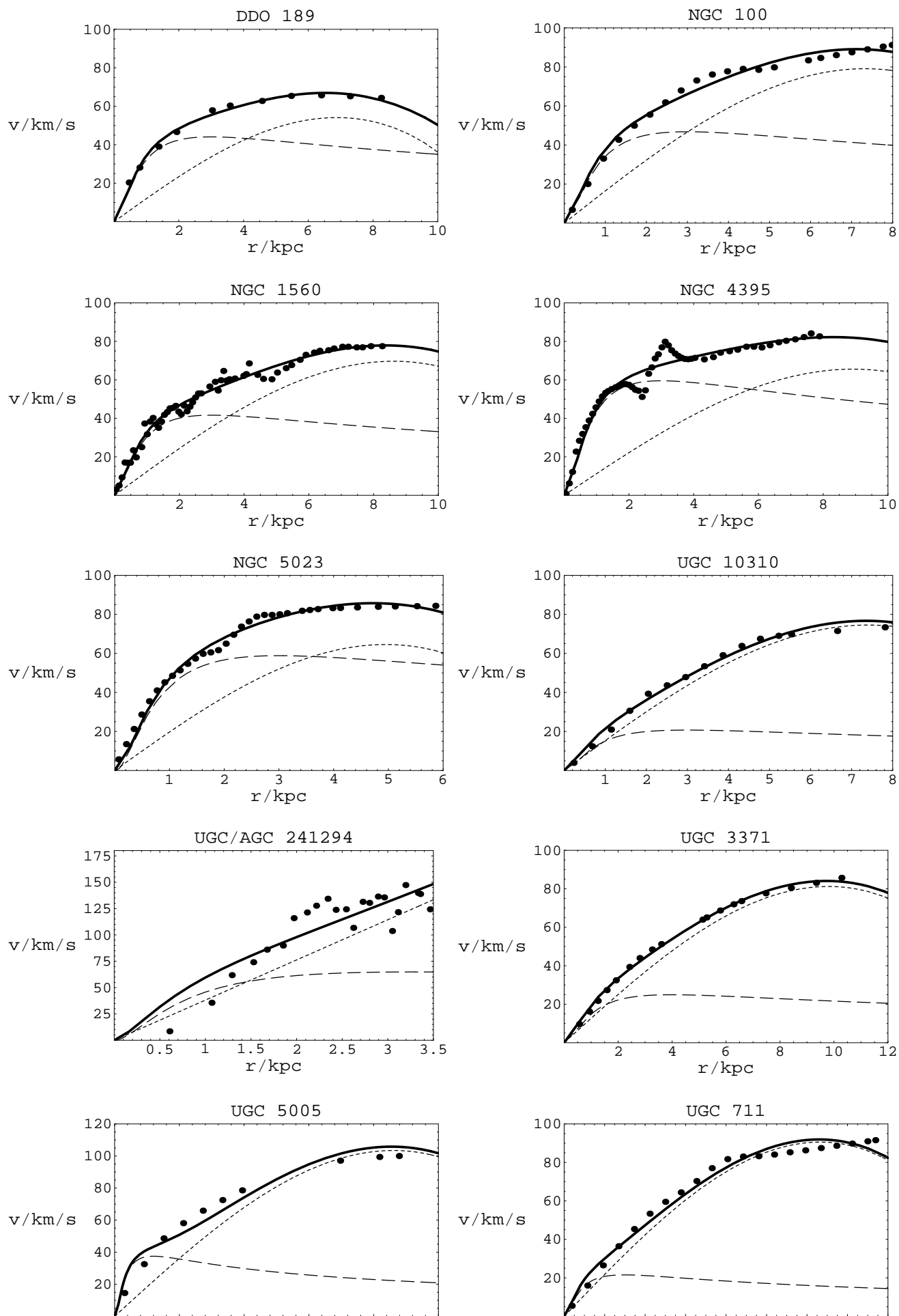
$$(\Delta\phi)_{BE} = 2|\phi(r_0) - \phi_\infty| - \pi, \quad (68)$$

where ϕ_∞ is the incident direction and r_0 is the coordinate radius of the closest approach to the center of the galaxy. Generally [36]

$$\phi(r_0) - \phi_\infty = \int_{r_0}^{\infty} e^{\frac{\lambda(r)}{2}} \left[e^{\nu(r_0) - \nu(r)} \left(\frac{r}{r_0} \right)^2 - 1 \right]^{-1/2} \frac{dr}{r}. \quad (69)$$

In the dimensionless variables introduced in Eqs. (56) we have

$$\phi(r_0) - \phi_\infty = \int_{\eta_0}^{\infty} \left[1 - \frac{2M_0(\eta)}{\eta} \right]^{-1/2} \left[e^{\nu(\eta_0) - \nu(\eta)} \left(\frac{\eta}{\eta_0} \right)^2 - 1 \right]^{-1/2} \frac{d\eta}{\eta}. \quad (70)$$



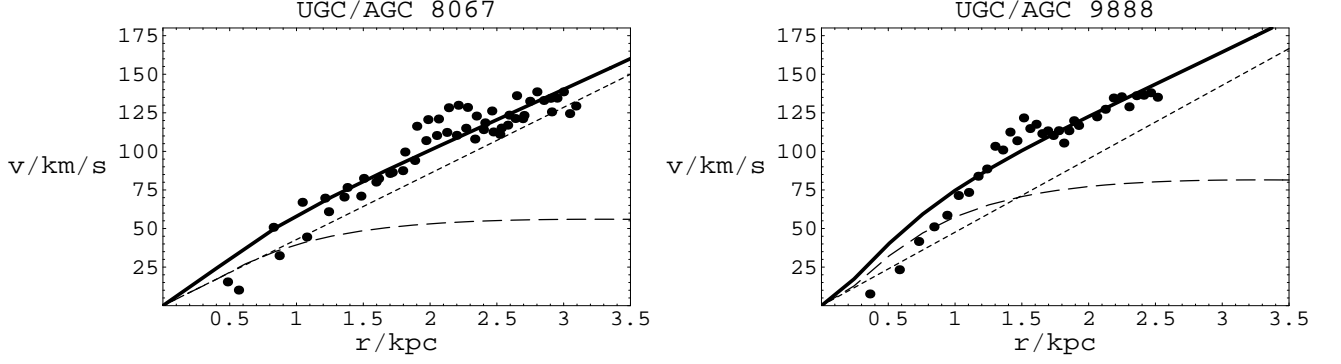


FIG. 5: Parametric fits of a sample of 12 galactic rotation curves from the data presented in [39] and [40]. The points represent the observational values. The solid curve is the rotation curve determined with the use of Eq. (67). The dotted curve represent the tangential velocity of the Bose-Einstein condensate, while the dashed curve is the Newtonian galactic rotation curve, corresponding to the presence of the normal baryonic matter in the galactic core.

We shall compare the values of the deflection angle Δ with a semi-realistic model for dark matter, in which it is assumed that the galaxy (the baryonic matter) is embedded into an isothermal mass distribution (the dark matter), with the density varying as $\rho = \sigma_v^2/2\pi Gr^2$, where σ_v is the line of sight velocity dispersion [1]. In this model it is assumed that the mass distribution of the dark matter is spherically symmetric. In fact, if the rotation curve is flat, then the mass distribution must be that of the isothermal sphere, for which we also have $v_{tg} = \sqrt{2}\sigma_v$. The surface density Σ of the isothermal sphere is $\Sigma(r) = \sigma_v^2/2Gr$. For this dark matter distribution the bending angle of light is constant and is given by $(\Delta\phi)_{DM} = 2\pi v_{tg}^2/c^2$ [42].

To compare the values of the deflection angle in the Bose-Einstein condensate and isothermal sphere dark matter models we introduce a dimensionless parameter Δ defined as

$$\Delta = \frac{(\Delta\phi)_{BE}}{(\Delta\phi)_{DM}} = \frac{(\Delta\phi)_{BE}}{2\pi (v_{tg}/c)^2}. \quad (71)$$

The variation of Δ as a function of the impact parameter r_0 is represented, for different values of the central density of the Bose-Einstein condensate dark matter, in Fig. 6.

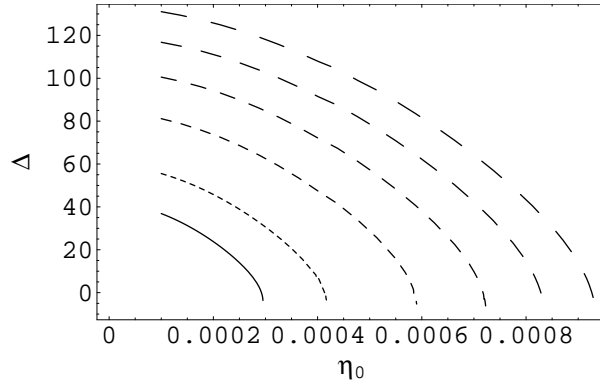


FIG. 6: The parameter Δ as a function of the impact parameter $\eta_0 = r_0/r^*$ for a Bose-Einstein condensate with $m = 5.6 \times 10^{-34}$ g and $a = 10^6$ fm, for different values of the central density: $\rho_{DM}^{(c)} = 10^{-27}$ g/cm³ (solid curve), $\rho_{DM}^{(c)} = 2 \times 10^{-27}$ g/cm³ (dotted curve), $\rho_{DM}^{(c)} = 4 \times 10^{-27}$ g/cm³ (short dashed curve), $\rho_{DM}^{(c)} = 6 \times 10^{-27}$ g/cm³ (dashed curve), $\rho_{DM}^{(c)} = 8 \times 10^{-27}$ g/cm³ (long dashed curve) and $\rho_{DM}^{(c)} = 10^{-26}$ g/cm³ (ultra-long dashed curve). In each case $v_{tg} = 300$ km/s.

Once the light deflection angle is known, one can study the gravitational lensing by the dark matter halos. The lensing geometry is illustrated in Fig. 7.

The light emitted by the source S is deflected by the lens L (a galaxy in our case) and reaches the observer O at an angle θ to the optic axis OL , instead of β . The lens L is located at a distance D_L to the observer and a distance

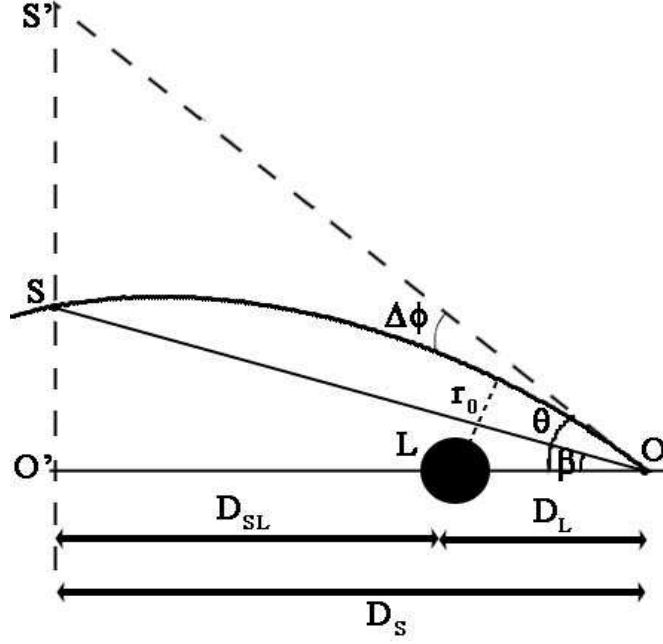


FIG. 7: The lensing geometry, showing the location of the observer O , of the lensing galaxy L and of the source S . The deflection angle is $\Delta\phi$. The angular diameter distances D_L , D_{LS} and D_S are also indicated.

D_{LS} to the source, respectively, while the observer-source distance is D_S . r_0 is the impact factor (distance of closest approach) of the photon beam.

The lens equation is given by [42]

$$\tan \beta = \tan \theta - \frac{D_{LS}}{D_S} [\tan \theta + \tan ((\Delta\phi)_{BE} - \theta)]. \quad (72)$$

By assuming that the angle θ is small, we have $\tan \theta \approx \theta$ and the lens equation can be written as

$$\beta \approx \theta - \frac{D_{LS}}{D_S} (\Delta\phi)_{BE}. \quad (73)$$

In the special case of the perfect alignment of the source, lens and observers, $\beta = 0$, and the azimuthal axial symmetry of the problem yields a ring image, the Einstein ring, with angular radius

$$\theta_E^{(BE)} \approx \frac{D_{LS}}{D_S} (\Delta\phi)_{BE}. \quad (74)$$

This equation can be expressed in a more familiar form by taking into account that the impact parameter $r_0 \approx D_L \theta$, which gives

$$\theta_E^{(BE)} \approx \sqrt{\frac{D_{LS}}{D_S D_L} \Delta\phi r_0} \approx \theta_E^{(GR)} \sqrt{\frac{r_0}{GM_B}} \sqrt{\Delta\phi}, \quad (75)$$

where $\theta_E^{(GR)}$ is the angular radius of the Einstein ring in the case of standard general relativity, $\theta_E^{(GR)} = \sqrt{4(D_{LS}/D_S D_L) GM_B}$, with M_B denoting the baryonic mass of the galaxy.

In the case of a galaxy with a heavy isothermal dark matter distribution, the Einstein radius of the lens formed in perfect alignment is [42]

$$\theta_E^{(DM)} = \left(\frac{4\pi\sigma_v^2}{c^2} \right) \frac{D_{LS}}{D_S}. \quad (76)$$

The ratio Δ of the Einstein's rings angular diameters in the brane world models and in the isothermal dark galactic halo model is

$$\Delta = \frac{\theta_E^{(BE)}}{\theta_E^{(DM)}} = \frac{(\Delta\phi)_{BE}}{2\pi (v_{tg}/c)^2}. \quad (77)$$

Therefore the ratio of the angular radii of the Einstein rings in the Bose-Einstein condensate dark matter model and in the isothermal dark matter model is given by the same parameter Δ which has been already introduced in Eq. (71). Hence the variation of the ratio of the Einstein rings in the two models can also be obtained from Fig. 6.

VIII. DISCUSSIONS AND FINAL REMARKS

Galactic rotation curves pose a challenge to present day physics and one would like to have a better understanding of some of their intriguing phenomena, like their universality and the very good correlation between the amount of dark matter and the luminous matter in the galaxy. In the present work we have considered, and further developed, an alternative view to the dark matter problem, namely, that the galactic rotation curves can be explained by models in which dark matter is in the form of a Bose-Einstein condensate. This assumption leads to a complete description of the basic properties of the dark matter condensates at both the Newtonian and general relativistic level, and gives a definite set of predictions which can be tested observationally. In particular, we have shown that the model provides a good descriptions for the galactic rotation curves by fitting our model to the data of 12 observed curves.

The numerical values of the basic parameters (mass and radius) of the condensed dark matter halos sensitively depend on the mass m of the condensate, on the scattering length a and on the central density $\rho_{DM}^{(c)}$, $R_{DM} = R(a, m, \rho_{DM}^{(c)})$, $M_{DM} = M_{DM}(a, m, \rho_{DM}^{(c)})$. Of course, in general, the values of the mass and radius of the gravitational condensate depend on the adopted model for the non-linearity.

The scattering length a is defined as the zero-energy limit of the scattering amplitude f [12]. Depending on the spin dependence of the underlying particle interaction, the scattering length may in general be also spin dependent. The spin independent part of the quantity is referred to as the coherent scattering length a_c . The scattering lengths can be obtained for some systems in the laboratory. In our estimations we have used the value of the scattering length obtained for dilute atomic Bose-Einstein condensates in terrestrial laboratory experiments. Another essential parameter is the mass m of the condensate particle, which, due to the lack of information about the physical nature of the dark matter, is a free parameter, which must be constrained by observations.

A powerful observational tool for discriminating between standard dark matter and Bose-Einstein condensate models is the study of the deflection of light (gravitational lensing) by the dark matter halos. Due to the fixed form of the galactic metric in the flat rotation curves region, in standard dark matter models the light bending angle is a function of the tangential velocity of particles in stable circular orbit and of the baryonic mass and radius of the galaxy. Generally, the specific form of the bending angle is determined by the galactic metric, and this form is very different for the Bose-Einstein condensate dark matter as compared to the other dark matter or modified gravity models (MOND [3], non-symmetric gravity [5], long-range self-interacting scalar fields [11] etc.).

The gravitational light deflection angle predicted by the Bose-Einstein condensate models is much larger than the value predicted by the standard dark matter approach. For example, there are significant differences in the lensing effect with respect to the isothermal dark matter halo model. Therefore the study of the gravitational lensing may provide evidence for the existence of the dark matter in the form of a Bose-Einstein condensate. Therefore, the study of the galaxy-galaxy lensing and of the dark matter halos' properties could provide strong constraints on the Bose-Einstein dark matter model and on related physical models.

In the present approach to dark matter all the relevant physical quantities can be obtained from observable parameters (the dark halo mass, the radius of the galaxy and the observed flat rotational velocity curves). Therefore this opens the possibility of testing the Bose-Einstein condensation models by using astronomical and astrophysical observations at the galactic-intergalactic scale. In this paper we have provided some basic theoretical tools necessary for the in depth comparison of the predictions of the condensate model and of the observational results.

Acknowledgments

The work of CGB was supported by research grant BO 2530/1-1 of the German Research Foundation (DFG). TH is supported by the RGC grant No. 7027/06P of the government of the Hong Kong SAR.

-
- [1] J. Binney and S. Tremaine, *Galactic dynamics*, Princeton University Press, Princeton (1987); M. Persic, P. Salucci and F. Stel, *Mon. Not. R. Astron. Soc.* **281**, 27 (1996); A. Boriello and P. Salucci, *Mon. Not. R. Astron. Soc.* **323**, 285 (2001).
- [2] R. H. Sanders, *Astron. Astrophys.* **136**, L21 (1984); R. H. Sanders, *Astron. Astrophys.* **154**, 135 (1986).
- [3] M. Milgrom, *Astrophys. J.* **270**, 365 (1983); J. Bekenstein and M. Milgrom, *Astrophys. J.* **286**, 7 (1984); M. Milgrom, *New Astron. Rev.* **46**, 741, (2002); M. Milgrom, *Astrophys. J.* **599**, L25, (2003); J. D. Bekenstein, *Phys. Rev. D* **70**, 083509 (2004).
- [4] P. D. Mannheim, *Astrophys. J.* **419**, 150 (1993); P. D. Mannheim, *Astrophys. J.* **479**, 659 (1997).
- [5] J. W. Moffat and I. Y. Sokolov, *Phys. Lett.* **B378**, 59 (1996); J. R. Brownstein and J. W. Moffat, *Astrophys. J.* **636**, 721 (2006); J. R. Brownstein and J. W. Moffat, *Mon. Not. R. Astron. Soc.* **367**, 527 (2006).
- [6] M. D. Roberts, *Gen. Rel. Grav.* **36**, 2423 (2004).
- [7] M. K. Mak and T. Harko, *Phys. Rev. D* **70**, 024010 (2004); T. Harko and M. K. Mak, *Annals Phys.* **319**, 471 (2005); T. Harko and K. S. Cheng, *Astrophys. J.* **636**, 8 (2005); C. G. Boehmer and T. Harko, arXiv:0705.2496 (2007).
- [8] V. V. Zhytnikov and J. M. Nester, *Phys. Rev. Lett.* **73**, 2950 (1994).
- [9] J. M. Overduin and P. S. Wesson, *Phys. Repts.* **402**, 267 (2004).
- [10] I. F. M. Albuquerque and L. Baudis, *Phys. Rev. Lett.* **90**, 221301 (2003).
- [11] J. W. Lee and I. G. Koh, *Phys. Rev.* **D53**, 2236 (1996); U. Nucamendi, M. Salgado and D. Sudarsky, *Phys. Rev. Lett.* **84**, 3037 (2000); T. Matos and F. S. Guzman, *Class. Quant. Grav.* **18**, 5055 (2001); U. Nucamendi, M. Salgado and D. Sudarsky, *Phys. Rev. D* **63**, 125016 (2001); A. Arbey, J. Lesgourgues and P. Salati, *Phys. Rev.* **D64**, 123528 (2001); A. Arbey, J. Lesgourgues and P. Salati, *Phys. Rev.* **D65**, 083514 (2002); L. G. Cabral-Rosetti, T. Matos, D. Nunez and R. A. Sussman, *Class. Quant. Grav.* **19**, 3603 (2002); J. E. Lidsey, T. Matos and L. Arturo Urena-Lopez, *Phys. Rev. D* **66**, 023514 (2002); A. Arbey, J. Lesgourgues and P. Salati, *Phys. Rev.* **D68**, 023511 (2003); J. P. Mbelek, *Astron. Astrophys.* **424**, 761 (2004); T. Matos, D. Nunez, R. A. Sussman, *Class. Quant. Grav.* **21**, 5275 (2004); A. Bernal and F. S. Guzman, *Phys. Rev.* **D74**, 103002 (2006); A. Bernal and F. S. Guzman, *Phys. Rev.* **D74**, 063504 (2006); F. S. Guzman and L. Arturo Urena-Lopez, *Astrophys. J.* **645**, 814 (2006); A. Arbey and F. Mahmoudi, *Phys. Rev.* **D75**, 063513 (2007); C. G. Boehmer and T. Harko, arXiv:0705.1756 (2007).
- [12] F. Dalfovo, S. Giorgini, L. P. Pitaevskii and S. Stringari, *Rev. Mod. Phys.* **71**, 463 (1999).
- [13] E. A. Cornell and C. E. Wieman, *Rev. Mod. Phys.* **74**, 875 (2002); W. Ketterle, *Rev. Mod. Phys.* **74**, 1131 (2002); L. Pitaevskii and S. Stringari, *Bose-Einstein condensation*, Clarendon Press, Oxford (2003); R. A. Duine and H. T. C. Stoof, *Phys. Repts.* **396**, 115 (2004); Q. Chen, J. Stajic, S. Tan and K. Levin, *Phys. Rept.* **412**, 1 (2005).
- [14] M. H. Anderson, J. R. Ensher, M. R. Matthews, C. E. Wieman and E. A. Cornell, *Science* **269**, 198 (1995); C. C. Bradley, C. A. Sackett, J. J. Tollett and R. G. Hulet, *Phys. Rev. Lett.* **75**, 1687 (1995); K. B. Davis, M. O. Mewes, M. R. Andrews, N. J. van Druten, D. S. Durfee, D. M. Kurn and W. Ketterle, *Phys. Rev. Lett.* **75**, 3969 (1995).
- [15] S. J. Sin, *Phys. Rev.* **D50**, 3650 (1994); S. U. Ji and S. J. Sin, *Phys. Rev.* **D50**, 3655 (1994).
- [16] W. Hu, R. Barkana and A. Gruzinov, *Phys. Rev. Lett.* **85**, 1158 (2000).
- [17] S. Khlebnikov, *Phys. Rev. A* **66**, 063606 (2002).
- [18] M. Nishiyama, M.-A. Morita and M. Morikawa, astro-ph/0403571 (2004).
- [19] F. Ferrer and J. A. Grifols, *JCAP* **0412**, 012 (2004).
- [20] J. A. Grifols, *Astropart. Phys.* **25**, 98 (2006).
- [21] T. Fukuyama and M. Morikawa, *Progress of Theoretical Physics* **115**, 1047 (2006); T. Fukuyama, M. Morikawa and T. Tatekawa, arXiv:0705.3091 (2007).
- [22] J. M. Whittaker, *Proc. Roy. Soc.* **A306**, 1 (1968)
- [23] A. D. Dolgov, A. Yu. Smirnov, *Phys. Lett. B* **621**, 1 (2005).
- [24] E. W. Mielke, B. Fuchs and F. E. Schunck, astro-ph/0608526 (2006).
- [25] J. Moffat, astro-ph/0602607 (2006).
- [26] J. Mielczarek, T. Stachowiak and M. Szydlowski, arXiv:0705.3017 (2007).
- [27] M. Yu. Khlopov, B. A. Malomed and Ya. B. Zeldovich, *Mon. Not. R. Astron. Soc.* **215**, 575 (1985); I. G. Dymnikova and M. Yu. Khlopov, *Mod. Phys. Lett.* **A15**, 2305 (2000); I. G. Dymnikova and M. Yu. Khlopov, *Eur. Phys. J.* **C20**, 139 (2001).
- [28] C. J. Short and P. Coles, *JCAP* **12**, 012 (2006); C. J. Short and P. Coles, *JCAP* **12**, 016 (2006); P. Coles and C. J. Spencer, *Mon. Not. R. Astron. Soc.* **342**, 176 (2003); P. Coles, *Mon. Not. R. Astron. Soc.* **330**, 421 (2002).
- [29] T. Padmanabhan, *Class. Quant. Grav.* **19**, 5387 (2002); T. Padmanabhan, *Int. J. Mod. Phys.* **D13**, 2293 (2004); A. Arbey, astro-ph/0506732; A. Arbey, *Phys. Rev.* **D74**, 043516 (2006); T. Padmanabhan, arXiv:0705.2533.
- [30] C. Barcelo, S. Liberati and M. Visser, *Class. Quant. Grav.* **18**, 1137 (2001).
- [31] E. B. Kolomeisky, T. J. Newman, J. P. Straley and X. Qi, *Phys. Rev. Lett.* **85**, 1146 (2000).
- [32] C. Barcelo, S. Liberati and M. Visser, *Living Rev. Rel.* **8**, 12 (2005).

- [33] X. Z. Wang, Phys. Rev. D **64**, 124009 (2001).
 [34] S. Chandrasekhar, *An introduction to the study of stellar structure*, Dover Publications, New York (1957).
 [35] S. Chandrasekhar, Mon. Not. R. Astron. Soc. **93**, 390 (1933).
 [36] S. Bharadwaj and S. Kar, Phys. Rev. D **68**, 023516 (2003).
 [37] T. Matos, F. S. Guzman and D. Nunez, Phys. Rev. **D62**, 061301 (2000).
 [38] N. K. Glendenning, *Compact Stars, Nuclear Physics, Particle Physics and General Relativity*, Springer, New York (2000).
 [39] W. J. G. de Blok and A. Bosma, Astron. Astrophys. **385**, 816 (2002).
 [40] K. Spekkens, R. Giovanelli and M. P. Haynes, Astron. J. **129**, 2119 (2005).
 [41] O. Y. Gnedin and J. R. Primack, Phys. Rev. Lett. **93**, 061302 (2004).
 [42] R. D. Blanford and R. Narayan, Annu. Rev. Astron. Astrophys. **30**, 311 (1992).

APPENDIX A: MOTION OF TEST PARTICLES

The motion of a test particle with four-velocity u^μ in the gravitational field of the galaxy can be described by the Lagrangian [7]

$$2L = \left(\frac{ds}{d\tau}\right)^2 = -e^{\nu(r)} \left(\frac{dt}{d\tau}\right)^2 + e^{\lambda(r)} \left(\frac{dr}{d\tau}\right)^2 + r^2 \left(\frac{d\Omega}{d\tau}\right)^2, \quad (\text{A1})$$

where $d\Omega^2 = d\theta^2 + \sin^2\theta d\phi^2$ and $d\tau = cdt$. From the Lagrange equations it follows that we have two constants of motion, the energy $E = e^{\nu(r)}\dot{t}$ and the angular momentum $l = r^2\dot{\phi}$ [37]. The condition $u^\mu u_\mu = -1$ gives $-1 = -e^{\nu(r)}\dot{t}^2 + e^{\lambda(r)}\dot{r}^2 + r^2\dot{\phi}^2$ and, with the use of the constants of motion we obtain

$$E^2 = e^{\nu+\lambda}\dot{r}^2 + e^\nu \left(\frac{l^2}{r^2} + 1\right). \quad (\text{A2})$$

This equation shows that the radial motion of the particles on a geodesic is the same as that of a particle with position dependent mass and with energy $E^2/2$ in ordinary Newtonian mechanics moving in the effective potential $V_{eff}(r) = e^{\nu(r)}(l^2/r^2 + 1)$. The conditions for circular orbits $\partial V_{eff}/\partial r = 0$ and $\dot{r} = 0$ lead to [37]

$$l^2 = \frac{1}{2} \frac{r^3 \nu'}{1 - \frac{r\nu'}{2}}, E^2 = \frac{e^\nu}{1 - \frac{r\nu'}{2}}. \quad (\text{A3})$$

The line element given by Eq. (47) can be rewritten in terms of the spatial components of the velocity, normalized with the speed of light, measured by an inertial observer far from the source, as $ds^2 = -c^2 dt^2 (1 - v^2/c^2)$ [7], where

$$\frac{v^2}{c^2} = e^{-\nu} \left[e^\lambda \left(\frac{dr}{cdt}\right)^2 + r^2 \left(\frac{d\Omega}{cdt}\right)^2 \right]. \quad (\text{A4})$$

For a stable circular orbit $\dot{r} = 0$, and the tangential velocity of the test particle can be expressed as

$$\frac{v_{tg}^2}{c^2} = \frac{r^2}{e^\nu} \left(\frac{d\Omega}{cdt}\right)^2. \quad (\text{A5})$$

In terms of the conserved quantities the angular velocity is given by

$$\frac{v_{tg}^2}{c^2} = \frac{e^\nu}{r^2} \frac{l^2}{E^2}. \quad (\text{A6})$$

With the use of Eqs. (A3) we obtain

$$\frac{v_{tg}^2}{c^2} = \frac{r\nu'}{2}. \quad (\text{A7})$$